

UNCLASSIFIED

AD 426835

DEFENSE DOCUMENTATION CENTER

FOR

SCIENTIFIC AND TECHNICAL INFORMATION

CAMERON STATION, ALEXANDRIA, VIRGINIA



UNCLASSIFIED

NOTICE: When government or other drawings, specifications or other data are used for any purpose other than in connection with a definitely related government procurement operation, the U. S. Government thereby incurs no responsibility, nor any obligation whatsoever; and the fact that the Government may have formulated, furnished, or in any way supplied the said drawings, specifications, or other data is not to be regarded by implication or otherwise as in any manner licensing the holder or any other person or corporation, or conveying any rights or permission to manufacture, use or sell any patented invention that may in any way be related thereto.

**Best
Available
Copy**

AEDC-TDR-63-242

426835



CATALOGED BY DDC

AS AD 110.

426835

SUMMARY OF ELECTRICAL PROPULSION DIAGNOSTIC INSTRUMENTATION

By

James B. Whited
Electrical Propulsion Group
Office of the Chief Scientist
ARO, Inc.

TECHNICAL DOCUMENTARY REPORT NO. AEDC-TDR-63-242

January 1964

Program Element 62405184/6950, Task 695006

(Prepared under Contract No. AF 40(600)-1000 by ARO, Inc.,
contract operator of AEDC, Arnold Air Force Station, Tenn.)

ARNOLD ENGINEERING DEVELOPMENT CENTER
AIR FORCE SYSTEMS COMMAND
UNITED STATES AIR FORCE

JAN 29 1964

NOTICES

Qualified requesters may obtain copies of this report from DDC, Cameron Station, Alexandria, Va. Orders will be expedited if placed through the librarian or other staff member designated to request and receive documents from DDC.

When Government drawings, specifications or other data are used for any purpose other than in connection with a definitely related Government procurement operation, the United States Government thereby incurs no responsibility nor any obligation whatsoever; and the fact that the Government may have formulated, furnished, or in any way supplied the said drawings, specifications, or other data, is not to be regarded by implication or otherwise as in any manner licensing the holder or any other person or corporation, or conveying any rights or permission to manufacture, use, or sell any patented invention that may in any way be related thereto.

SUMMARY OF ELECTRICAL PROPULSION
DIAGNOSTIC INSTRUMENTATION

By
James B. Whited
Electrical Propulsion Group
Office of the Chief Scientist
ARO, Inc.
a subsidiary of Sverdrup and Parcel, Inc.

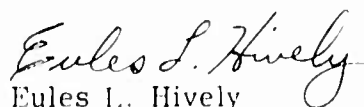
January 1964


ABSTRACT

This report summarizes the instrumentation development effort that was initiated at the Arnold Engineering Development Center to effect plasma diagnostics during the long-term testing of electrical propulsion systems. Two different ion beam sources were instrumented to obtain the basic properties of the plasma, such as the electron temperature, electron and ion densities, and the space charge potentials. The basic instrumentation required to effect preliminary diagnostics are the "plasma eater," the positive ion probe, the Langmuir double probe, the Faraday cup, and the emissive probe. With these devices, it is possible to obtain both integral and differential measurements of the beam characteristics. Analysis of the data is also included.

PUBLICATION REVIEW

This report has been reviewed and publication is approved.


Eules L. Hively
Acting Chief, Propulsion Division
DCS/Research


Donald R. Eastman, Jr.
DCS/Research

CONTENTS

| | <u>Page</u> |
|---|-------------|
| ABSTRACT | iii |
| NOMENCLATURE | vii |
| 1.0 INTRODUCTION | 1 |
| 2.0 BASIC INSTRUMENTATION | |
| 2.1 Plasma Eater | 2 |
| 2.2 Positive Ion Beam Probe | 4 |
| 2.3 Langmuir Double Probe | 5 |
| 2.4 Faraday Cup | 7 |
| 2.5 Emissive Probe | 10 |
| 3.0 SUMMARY OF RESULTS AND CONCLUSION | 11 |
| REFERENCES | 12 |

ILLUSTRATIONS

Figure

| | |
|---|----|
| 1. Argon Discharge System Apparatus | 13 |
| 2. Lithium Ion Gun | |
| a. End View | 14 |
| b. Three-Quarter View | 15 |
| 3. Lithium Discharge System | 16 |
| 4. Plasma Eater | 17 |
| 5. Plasma Eater Characteristics | 18 |
| 6. General Potential Diagram between Plates | 19 |
| 7. $\frac{\sum i_p}{i_{e2}} - 1$ vs Probe Voltage | 20 |
| 8. Positive Ion Probe | 21 |
| 9. Positive Ion Probe Characteristics | 22 |
| 10. Floating Double Probe Circuit | 23 |
| 11. Volt-Ampere Characteristic; Double Probe | 24 |
| 12. Faraday Cup | 25 |
| 13. Faraday Cup Biasing | 26 |

| <u>Figure</u> | <u>Page</u> |
|---|-------------|
| 14. Chamber Grounded | |
| a. Neutralizer On. | 27 |
| b. Neutralizer Off. | 28 |
| 15. Chamber Floating | |
| a. Neutralizer On. | 29 |
| b. Neutralizer Off. | 30 |
| 16. Sample Potential Distribution. | 31 |
| 17. Possible Potential Solutions, Eqs. (18) and (19). | 32 |
| 18. Graphical Solution of Emissive Probe Data. | 33 |

NOMENCLATURE

| | |
|-----------|---|
| A | Area, cm^2 |
| a | Point where virtual cathode forms |
| e | Electron charge, 1.6×10^{-19} coulombs |
| I | Current, amp |
| i_e | Electron current, amp |
| i_p | Ion current, amp |
| J_0 | Electron space current |
| K | Boltzmann's constant, 1.38×10^{-16} $\frac{\text{ergs}}{^\circ\text{K}}$ |
| M_e | Mass of an electron, gm |
| M_p | Mass of an ion, gm |
| N_e | Electron density, particles/ cm^3 |
| N_i | Ion density, particles/ cm^3 |
| T_e | Electron temperature, $^\circ\text{K}$ |
| T_p | Ion temperature, $^\circ\text{K}$ |
| t | Time, sec |
| V | Voltage, volts |
| V_0 | Electrostatic potential at $x = 0$ |
| V_1 | Electrostatic potential at $(a - x) = 2x - a$ |
| V_2 | Electrostatic potential at $(2x - a) = x = 2x$ and $0 \leq x \leq a$ |
| V_c | Contact potential, volts |
| V_d | Probe voltage, volts |
| V_f | Floating potential, volts |
| v | Velocity, cm/sec |
| x | 1/2 Beam width-cm |
| λ | Quantity $\left[\frac{\sum i_p}{i_{e2}} - 1 \right]$ |
| ρ | Net charge density |
| α | $\frac{\lambda_1 J_{01}}{\lambda_2 J_{02}} \exp(\phi V_c)$ |
| ϕ | $\frac{e}{KT_e}$ |

1.0 INTRODUCTION

The basic objectives of the instrumentation research by the Electrical Propulsion Group* are to develop electrical propulsion diagnostic measuring and monitoring techniques in addition to establishing standard procedures for calibration. These research efforts depend materially on the information now obtained through the use of techniques and devices established by this program.

Two basic ion sources were constructed for the preliminary studies. The oscillating electron ion gun is a modified mass spectrometer source that was obtained from Oak Ridge National Laboratories. The gun consists of a filament providing an electron beam, oscillating in a magnetic field, which bombards and hence ionizes the gas. The positive ions are collimated and extracted by means of slits in the acceleration plates. Argon gas was initially selected because of its high mass and high probability of being singly ionized. The operating system is shown in Fig. 1.

Measured plasma properties included electron temperatures, charged particle densities, and space potentials. Problems of relating plasma properties to axial distance could not be resolved because the argon flow could not be stringently regulated. In addition, the flow had to be interrupted to relocate instruments along the axis of the small research cell.

A lithium ion gun was also designed and constructed to be used as a reliable ion source, producing singly ionized particles that were relatively free of neutrals. The ion gun was constructed from a one-inch by one-inch platinum mesh filament and coated with Beta-eucryptite ($\text{Li}_2\text{O} \cdot \text{Al}_2\text{O}_3 \cdot 2\text{SiO}_2$). Three accelerating and focusing plates were mounted between the filament and the neutralizer—a tungsten wire encircling the exit aperture. The device is shown in Figs. 2a and b. The first accelerating plate was connected electrically to the emitter filament and was maintained at filament potential, approximately 1,000 volts above ground. The second plate was biased in the range of 200 to 300 volts negative. The exit plate was tied to ground.

The Beta-eucryptite coating on the platinum filament was fused to a glossy solid condition by heating to a temperature of approximately

*Office of the Chief Scientist, ARO, Inc., Arnold Engineering Development Center (AEDC), Air Force Systems Command (AFSC).

Manuscript received October 1963.

1500°C for several minutes at pressures below 10^{-4} torr. The acceleration plates were optically aligned by drilling all exit holes simultaneously. The accel-decel scheme was used with a maximum acceleration of 1,000 volts and a minimum deceleration potential of approximately 200 volts, to prevent electrons from bombarding the ion filament. A beam of several hundred microamperes was obtained using this source at a filament temperature of approximately 1300°C.

The basic research cell, a 25-inch-long by six-inch by six-inch cross section, was maintained in the 10^{-9} torr region during all operations. This system is shown in Fig. 3.

A three-directional, probe traverse stand was assembled, and a removable plexiglass top allowed observation of engine operation and probe movements. Position repeatability was satisfactory for initial research applications using only optical alignment. Over 90 percent of the cell volume could be probed. The properties measured in the plasma beam included charged particle distribution and densities, electron temperatures, and plasma potentials.

2.0 BASIC INSTRUMENTATION

2.1 PLASMA EATER

2.1.1 Discussion

One of the basic instruments used in the experiments to measure the rate of flow of a plasma discharge is the "plasma eater" (Ref. 1). The device consists of alternately connected, closely spaced, metal plates and is shown in Fig. 4. In our experiments, the plasma eater was used both as a collector and a double Langmuir probe. The large collecting area in a small volume enabled the recording of stable and repeatable volt-ampere characteristics of the relatively low-density argon discharge. The simple circuit used to obtain the characteristics is also shown in Fig. 4. Figure 5 shows a typical volt-ampere characteristic curve obtained from the probe. Analysis of the characteristics follows the technique previously developed (Ref. 2). Since detailed theoretical background for the use of the floating double probe is available, in the reference, only a brief introduction to this theory will be discussed.

2.1.2 Analysis of Data

If a Maxwell-Boltzmann velocity distribution is assumed, the expression for the total positive ion current reaching each plate is given by

$$\Sigma i_p = i_{e1} + i_{e2} \\ A_1 i_{e1} \exp\left(-\frac{V_1}{kT_e}\right) + A_2 i_{e2} \exp\left(-\frac{V_2}{kT_e}\right) \quad (1)$$

where A_1 and A_2 represent the sum of the collecting areas of the two sets of plates, i_{e1} and i_{e2} represent the respective electron currents, V_1 and V_2 equal the respective plate voltages with respect to the plasma, and T_e is the electron temperature. The potential distribution between two adjacent plates is shown in Fig. 6. Since the sum of voltages around a closed loop equals zero,

$$V_1 + V_3 - V_2 - V_4 = 0 \quad (2)$$

Combining this result with the equation for Σi_p and taking the logarithm yields

$$\ln\left(\frac{\Sigma i_p}{i_{e2}} + 1\right) = -\phi A_2 + \ln a \quad (3)$$

where

$$\phi = \frac{e}{kT_e}$$

and

$$a = \frac{A_1 i_{e1}}{A_2 i_{e2}} \exp(-\phi V_1)$$

This is an equation of a straight line when plotted on semi-log paper. A plot of $\frac{\Sigma i_p}{i_{e2}} + 1$ vs V_d has a slope of $-\frac{e}{kT_e}$, thus determining T_e directly. Figure 5 shows a typical volt-ampere characteristic from which values of $\frac{\Sigma i_p}{i_{e2}} + 1$ were obtained and plotted in Fig. 7. The slope yields an electron temperature of 162,000°K. The electron temperature was also calculated by the equivalent resistance method (Ref. 2). Equation (3) may be written as:

$$\frac{\Sigma i_p}{i_{e2}} = a \exp(-\phi V_d) + 1 \quad (4)$$

Differentiating i_{e2} with respect to V_d and evaluating at $V_d = 0$ yields

$$\left. \frac{di_{e2}}{dV_d} \right|_{V_d=0} = \frac{\Sigma i_p - \phi a}{(a + 1)^2} \quad (5)$$

Solving for T_e and substituting, $\frac{dV_d}{dI_d} = \frac{dV_d}{dI_e}$

$$I_e = 11,600 \frac{e}{(kT_e + 1)^{3/2}} \left(\sum I_p \frac{dV_d}{dI_d} \right) \quad V_d = 0$$

$$\text{Let } G = \frac{1}{1 + e^{-x}} \quad (6)$$

then

$$I_e = 11,600 (G + G^2) \left(\sum I_p \frac{dV_d}{dI_d} \right) \quad V_d = 0$$

$$I_e = 11,600 (G + G^2) (R_0 \sum I_p) \quad \text{where } R_0 = \left. \frac{dV_d}{dI_d} \right|_{V_d=0}$$

$R_0 = 2.22 \times 10^{-8}$ ohms, and $T_e = 163,000^\circ\text{K}$, which agrees quite well with results from the semi-log plot. From electron temperature and probe geometry, ion density and floating potential can be calculated:

$$V_p = - \frac{kT_e}{2e} \ln \left[\frac{I_e M_p}{I_i M_e} \right] = 200 \text{ volts} \quad (7)$$

$$N_i = \frac{1.34 \times 10^{22}}{A_p} I_p \left[\frac{M_i}{I_i} \right] = 1.3 \times 10^{17} \frac{\text{ion}}{\text{cm}^3} \quad (8)$$

where

$$A_p = 93 \text{ cm}^2$$

For several argon flow rates and probe positions, ranges of electron temperature and densities were determined as 75,000 to 225,000°K and 10^4 to 10^8 ion/cm³, respectively, with a total acceleration of 600 volts.

Axial plots of electron temperature would have been useful in defining the plasma discharge, but they could not be accurately made because of poor regulation of the argon flow.

2.2 POSITIVE ION BEAM PROBE

The positive ion probe (Ref. 3), as shown in Fig. 8, consists of Beta-eucryptite fused on a strip of platinum gauze, two focusing grids, and a collector plate. Representative plots of collector current as a function of the acceleration potential are shown in Fig. 9. With the plasma present, there is negligible ion transmission until V_{\min} is

attained. At this point, there is a rapid increase in transmission until V_{max} is reached, where collector current is the same as with no plasma present. The plasma potential is taken as the value of acceleration potential where the half maximum collector current is transmitted.

The maximum collector current with plasma present was increased above the expected value when runs were made at pressures above 10^{-4} torr. This observed characteristic was probably caused by increased ionization of background gases. To ensure that the collector shielding of the ion probe was adequate, the following procedure was used before each test run. The argon ion flow was established, and the positive ion probe operated as usual throughout the acceleration potential range, but with the probe heater current off. Negligible collector current was observed. The range of plasma potential for these experiments was from 100 to 220 volts. The most reproducible volt-ampere characteristics were made at lower pressures, lower plasma densities, and thus lower plasma potentials.

2.3 LANGMUIR DOUBLE PROBE

2.3.1 Discussion

A semi-automatic, Langmuir, double probe circuit was also used in probing the discharge (Fig. 10). The problem of isolating the floating circuitry from ground was solved to a degree that ion current compensation was not necessary. Since the double probe plates were subject to ionic bombardment while a volt-ampere characteristic was being made, the "ion current" leakage to ground resulted in a zero shift. However, this shift was minimized by careful shielding and isolation of the floating circuit and was dialed out in the XY plotter. Instruments (I) and (V) were Keithly Model 600A electrometers. A₁ and A₂ were Dynamics Model 3140 d-c isolation amplifiers. To obtain a volt-ampere characteristic, S₁ was held closed momentarily and then released, providing an exponentially decaying voltage sweep from +150 to -150 volts with a time constant of approximately 3 seconds. While the time of the voltage sweep should be kept as short as possible, noticeable a-c current was passed through the capacitive geometric arrangement of the plates at higher sweep rates. A typical characteristic is shown in Fig. 11.

2.3.2 Analysis of Data

The basic relations facilitating analyses to obtain plasma properties from this example are as shown on the following page.

Electron temperature:

$$T_e = 11,600 (G + G^2) R_m \Sigma i_p \left\{ \begin{array}{l} \text{equivalent} \\ \text{resistance} \\ \text{method} \end{array} \right\} \quad (9)$$

where

$$G = \left[\frac{\Sigma i_{e2}}{\Sigma i_p} \right] V_{te} = 0 \quad (10)$$

R_m , i_{e2} , and Σi_p are shown in Fig. 11

$$T_e = 70,500 \text{ K}$$

Using the approximate expression for floating potential, V_f (with respect to space potential),

$$V_f = - \frac{k T_e}{e} \ln \left[\frac{1_e M_p}{M_e T_p} \right] \quad (11)$$

where

T_e has been calculated,

T_p is taken as the emission temperature of Beta-eucryptite, approximately 1700°K

M_p is a mass of a lithium atom

Thus,

$$V_f = - \frac{1.38 \times 10^{-23} \times 7.85 \times 10^4}{2 \times 1.6 \times 10^{-19}} \ln \frac{7.85 \times 10^4 \times 1.5 \times 10^{-26}}{1.7 \times 10^3 \times 9.1 \times 10^{-31}} \quad (12)$$

69 volts

Ion density is

$$N_i = \frac{Q}{As} \psi^2 \left[\frac{M_p}{1_p} \right]^{1/2} \quad (13)$$

where

As is taken as the area of the rectangular plates, approximately 0.405 cm²

i_{e2} , as before, is 11×10^{-11} amp

ψ is an accumulative constant = 1.34×10^{27}

Thus,

$$N_i = \frac{1.34 \times 10^{27}}{0.405} (1.1 \times 10^{-10}) \left(\frac{1.15 \times 10^{-26}}{1.7 \times 10^{-31}} \right)^{1/2} \quad (14)$$

$= 3.42 \times 10^4 \frac{\text{ion}}{\text{cm}^3}$

Volt-ampere characteristics were repeatable if the plasma source was not altered.

2.4 FARADAY CUP

2.4.1 Discussion

Faraday cups are small "point" collectors. They consist of an enclosure with a small opening point toward the discharge arc containing several biasing grids so that a particular charged particle can be detected on a collecting plate.

A Faraday cup was designed and constructed to measure ion densities directly, and also to serve as an indication of neutral particles in the beam. The schematic of the Faraday cup is shown in Fig. 12. The No. 1 screen was biased to suppress electron entrance to the cup. The No. 2 screen was biased to suppress secondaries from the first plate. Ion impingement was monitored through an electrometer at the first plate. The diameter of the device was 3/8 inch, and the length was 3/4 inch.

2.4.2 Analysis of Data

Calculation of ion density is shown below:

$$eV = \frac{1}{2} Mv^2$$

or

$$v = \sqrt{\frac{2eV}{M}}$$

$$v = 5.28 \times 10^5 \sqrt{V} \quad \frac{\text{cm}}{\text{sec}} \quad (15)$$

where

M = mass of lithium ion = 1.5×10^{-26} kilograms

Area of the entrance aperture = $2.15 \times 10^{-2} \text{ cm}^2$

Since

$$N_i = \frac{I}{vAc}$$

$$\sqrt{V} = 5.28 \times 10^5 \times 2.15 \times 10^{-2} \times 1.6 \times 10^{-19} \quad (16)$$

then

$$N_i = \frac{I}{\sqrt{V}} = (5.5 \times 10^{14}) \frac{\text{ion}}{\text{cm}^3}$$

For the above example, where the Langmuir, double probe, volt-ampere characteristic was analyzed, the Faraday cup was located in the same neighborhood of the double probe plates. The collector current was 4.2×10^{-9} amp, and the acceleration voltage was 225 volts. Thus,

$$N_i = \frac{4.2 \times 10^{-9} \times 3.5 \times 10^{14}}{\sqrt{225}} = 15.4 \times 10^4 \frac{\text{ion}}{\text{cm}^2} \quad (17)$$

While this value is almost an order of magnitude larger than the calculated double probe value, it is felt that the agreement is good considering the accuracies of the measured parameters, the slight difference in location of the two devices, and the finite time required to obtain the double probe characteristic. Since collection of the Faraday cup can be varied through certain bias ranges of the two control screens, the calibration technique for proper use of this collector is given below.

In Fig. 13 a range of voltage was applied to the suppressor screen for several discrete negative voltages on the electron suppressor screen (No. 1). The bias combination that resulted in constant collection on the No. 1 plate was selected as the proper bias arrangement for direct ion current measurement. The impingement on the No. 1 and No. 2 screens was observed to be negligible compared to the ion current at the No. 1 plate (2 orders of magnitude).

An attempt was made to measure neutrals in the beam with the Faraday cup. The No. 2 and No. 1 screens were biased positively and negatively, respectively, until negligible collection was made on the first plate. The tungsten wire was then brought to emission temperature and collection was observed on the second plate, which was biased negatively approximately 10 volts. This collection was a result of ionization of the residue gas and was not noticeably changed when the discharge was interrupted. This observation indicated that there was a very small percentage of neutrals in the discharge.

The gross effect of beam neutralization by electron injection has been observed. The 25- x 6- x 6-inch vacuum chamber was electrically floating from ground. Four steady-state modes of operation were investigated: floating the chamber with the neutralizer on and off, and grounding the chamber with the neutralizer on and off.

The results of sweeping the discharge with the Faraday cup in these four modes of operation are shown in Figs. 14 and 15. For these collections, the No. 1 plate was biased approximately 10 volts positively, to cause a return of secondary electrons. The No. 1 and No. 2 screens were floating, and the outer shield was floating for all applications of the Faraday cup.

In a treatment of the problem of time-independent mixing for the injection of electrons with an initial velocity distribution (Ref. 4), a solution is offered for ion and electron distributions across a slab of a discharge where electrons have been emitted at the edge of the ion beam immediately after acceleration of the ions.

$$\frac{dV_1}{d\mu} = \frac{1}{\pi} \int_{-\infty}^{\infty} \frac{N_0}{N_1} \exp(-V_1^2) \left(\frac{V_1^2}{V_2^2} \right) \exp(-V_2^2) dV_2 = 1 \quad (18)$$

for $0 \leq V_1 \leq \Delta$ and $(\Delta - a) \leq V_1 \leq \Delta$

$$\frac{dV_2}{d\mu} = \frac{N_0}{N_1} \exp(-V_2^2) \exp(-V_2^2) = 1 \quad (19)$$

for $0 \leq V_2 \leq a$ and $(\Delta - a) \leq V_2 \leq \Delta$

where 2Δ = total width of beam (see Fig. 16).

There are four general types of solutions for these equations, and these results are repeated in Fig. 17. Solution 1 always applies when N_0/N_1 is less than 1. Solution 2 is unstable, being critically dependent on initial beam width. As N_0/N_1 becomes greater than 1, Solutions 1, 2, 3, or 4 can apply. Solution 3 is shown as a double mode solution to demonstrate that higher mode solutions are possible. Solution 4 is a stable mode but may decay into a Type 1 or Type 3 solution and should be termed only marginally stable. It is also shown that there exists a maximum value of N_0/N_1 beyond which a Type 1 solution cannot exist.

The Faraday cup has been previously described as being used as a point collector to make calorimetric measurements throughout the discharge region during the four modes of floating and grounding the chamber, with and without the use of the neutralizer. This technique is crude in that no absolute values can be established for ion and/or electron number densities. However, the results predicted by the research group of NASA (Ref. 4), described above, and the efficiency of the neutralization scheme could be observed by this technique. The results of sweeping the discharge with the Faraday cup in these four modes of operation are shown in Figs. 14 and 15. Comparing the results in Figs. 14a and b shows that in the grounded environment the ion beam is broadened when electrons for neutralization must be provided from secondaries from ground or charge exchange through the residue gas as in Fig. 14b. Figures 14a and 15a show the third solution of Eqs. (18) and (19) and show a marked dependence of the ion beam on the neutralizer to establish a discharge with densities comparable to those in a grounded environment when compared to Fig. 15b.

2.5 EMISSIVE PROBE

The emissive probe used was a 1/8-inch, five-mil tungsten wire exposed through the end of a double hole ceramic tube. The element was brought to emission temperature and a variable positive potential applied. With this potential at zero and the element at emission temperature within the plasma, the element emits electrons to the positive space potential. As the voltage on the emissive element is increased, the emission remains limited until the plasma potential is approached where it passes to space charge limited emission and goes to zero as the applied voltage equals the space potential.

The introduction of electrons into the plasma stream can, of course, affect the neutralization of the discharge and quite possibly alter the mode of the discharge, that is, from Solution 1 to Solution 3 of Eqs. (18) and (19). For these reasons, the emission was held at least one order of magnitude below the N_0 or N_1 of Eqs. (18) and (19). Thus, the positive section of the volt-ampere curve normally obtained with a single Langmuir probe was obtained in the same order of magnitude as the emission of electrons. Therefore, this Langmuir current was obtained with the emissive probe with the element not at emission temperature, but with some heater current just below an emissive value in an effort to preserve a constant work function of the collecting element. A typical graphical solution for plasma potential using the emissive probe is shown in Fig. 18.

An approximation of the floating potential is obtained if the logarithm of curve C is plotted and the asymptotes are drawn through the emission limited and the space charge limited regions. There has been no criterion set on emission temperatures of the emissive probe; therefore, a variation of heater current to the probe would shift the intersection of these asymptotes appropriately.

An experiment was performed to determine the degree of correlation possible between space potential measurements with the positive ion probe and differential space potential measurements with the use of an emissive probe. The lithium ion probe yields a measurement of the maximum positive potential (ϕ_{\max} in Fig. 16) that the ions must traverse in order to be collected. Location of this point in any cross-sectioned slab is uniquely determined by use of the Faraday cup described above. From the emissive probe, one obtains the local space potential in the neighborhood of the emissive element.

The positive ion probe was employed just before and just after the sampling with the emissive probe and with the emissive probe removed

from the area of this cross section. Although there were several minutes of time between the samplings with the positive ion probe, the characteristics were repeatable with a variation of 5 percent measuring a maximum potential in the beam of approximately 160 volts. The reduced data of the emissive probe indicated a potential of approximately 150 volts. Runs were made through the day, and values were taken at a cross section approximately three and a half inches from the source, with a discharge of approximately 75 milliamperes net into the grounded chamber with the neutralizer off and an acceleration of 700 volts. These sample values were repeatable with a variation of approximately 10 percent.

3.0 SUMMARY OF RESULTS AND CONCLUSION

Two different sources of direct-current plasma discharges have been investigated. The instrumentation of these discharges was directed toward familiarization and development of "standard" measuring techniques and methods of analysis. The most encouraging developments were the degrees of correspondence obtained between different probes monitoring the same plasma property. The correlation of Langmuir probe and Faraday cup measurements of ion density is thought to be quite acceptable, considering the individual accuracy and reliability of each instrument.

Both devices are limited in their usefulness in probing very dense and energetic ionized discharges because of loss of the probe material. Of course, any probe that must be placed within the discharge will disturb the plasma flow by particle interception and by field interaction, thereby possibly changing the properties that the probe is attempting to measure.

The correspondence between the emissive probe and positive ion probe in the measurement of the maximum beam potential is thought to be most worthwhile since by the use of the positive ion probe, a plasma property and the general behavior of the discharge can be observed without the introduction of a foreign material into the beam. The possible problem of particle interaction with the use of the positive ion probe is now being investigated.

The lithium source and its vacuum system will be operated as an instrument calibration rig. It is felt that a valuable experiment has been established where plasma properties are measured by several devices and correlation of these properties can be made to an

acceptable degree. Any new technique or device that will be developed for use in beam studies can be evaluated by comparison to measurements made by the instruments discussed in this report.

REFERENCES

1. Alexeff, I. and Neidigh, R. V. "The Plasma Eater: A Device to Measure the Rate of Flow of a Plasma." ORNL-3246, February 1962.
2. Johnson, E. O. and Malter, L. "A Floating Double Probe Method for Measurements in Gas Discharges." Physics Review, Vol. 80, No. 1, October 1950, pp. 58-63.
3. Haste, G. R. and Barnett, C. F. "Plasma Potential Measurements Using an Ion Beam Probe." Journal of Applied Physics, Vol. 33, No. 4, April 1962, p. 1397-1399.
4. Seitz, R. N., Shelton, R. D., and Stuhlinger, F. "Present Status of the Beam Neutralization Problem." Presented at the ARS Electrostatic Propulsion Conference, U. S. Naval Postgraduate School, Monterey, Calif., November 3-4, 1960 (Preprint # 1381-60).

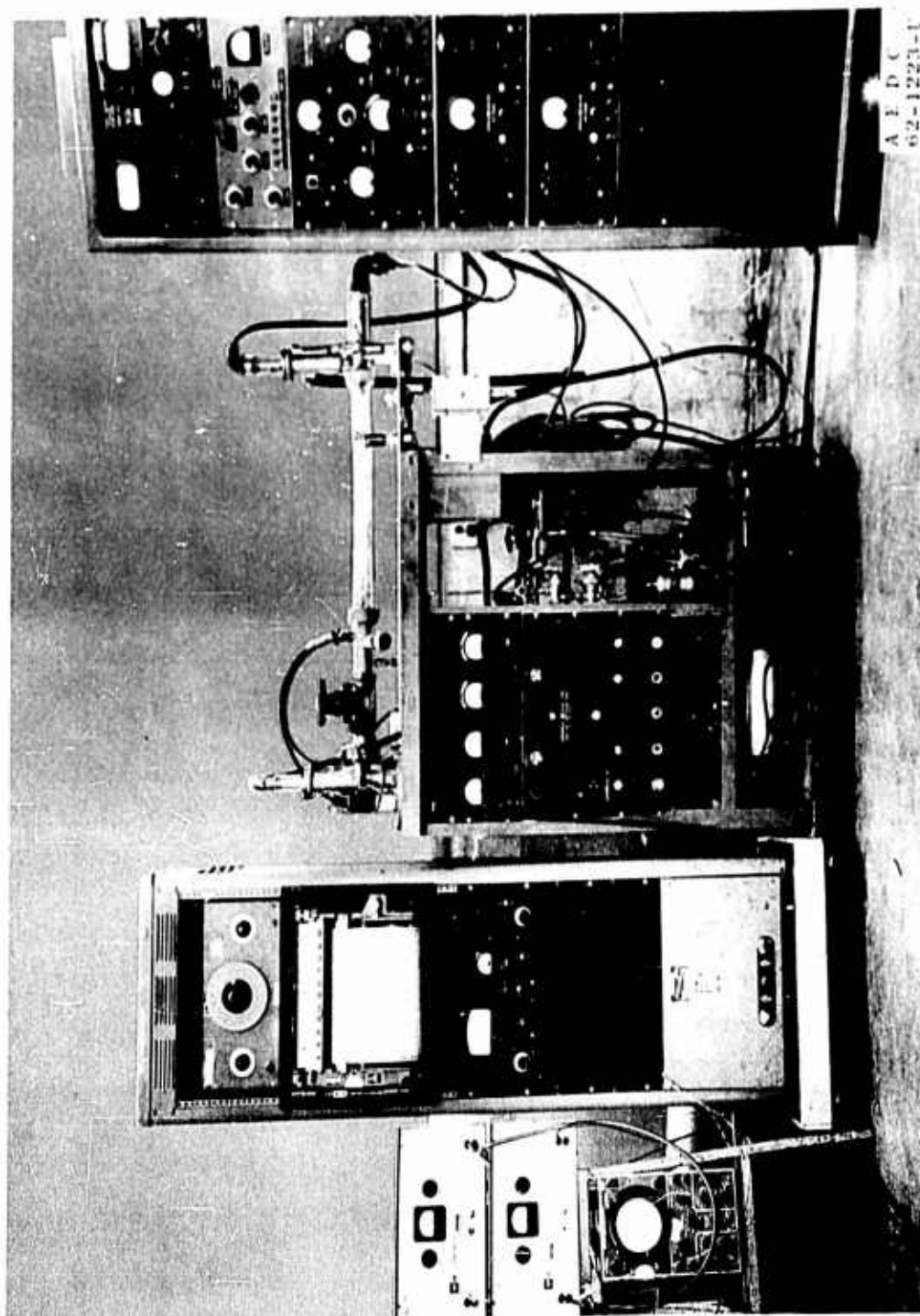
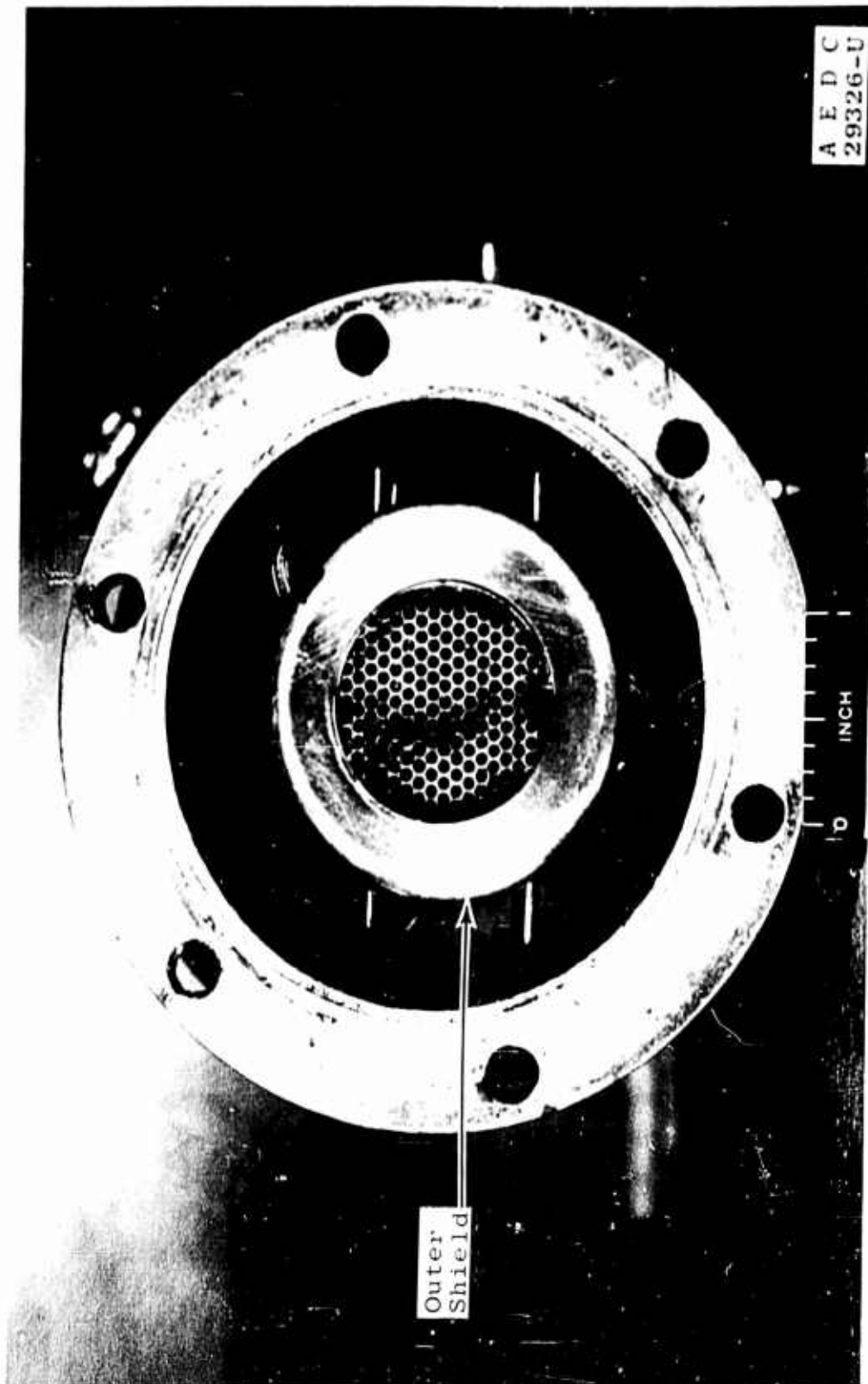
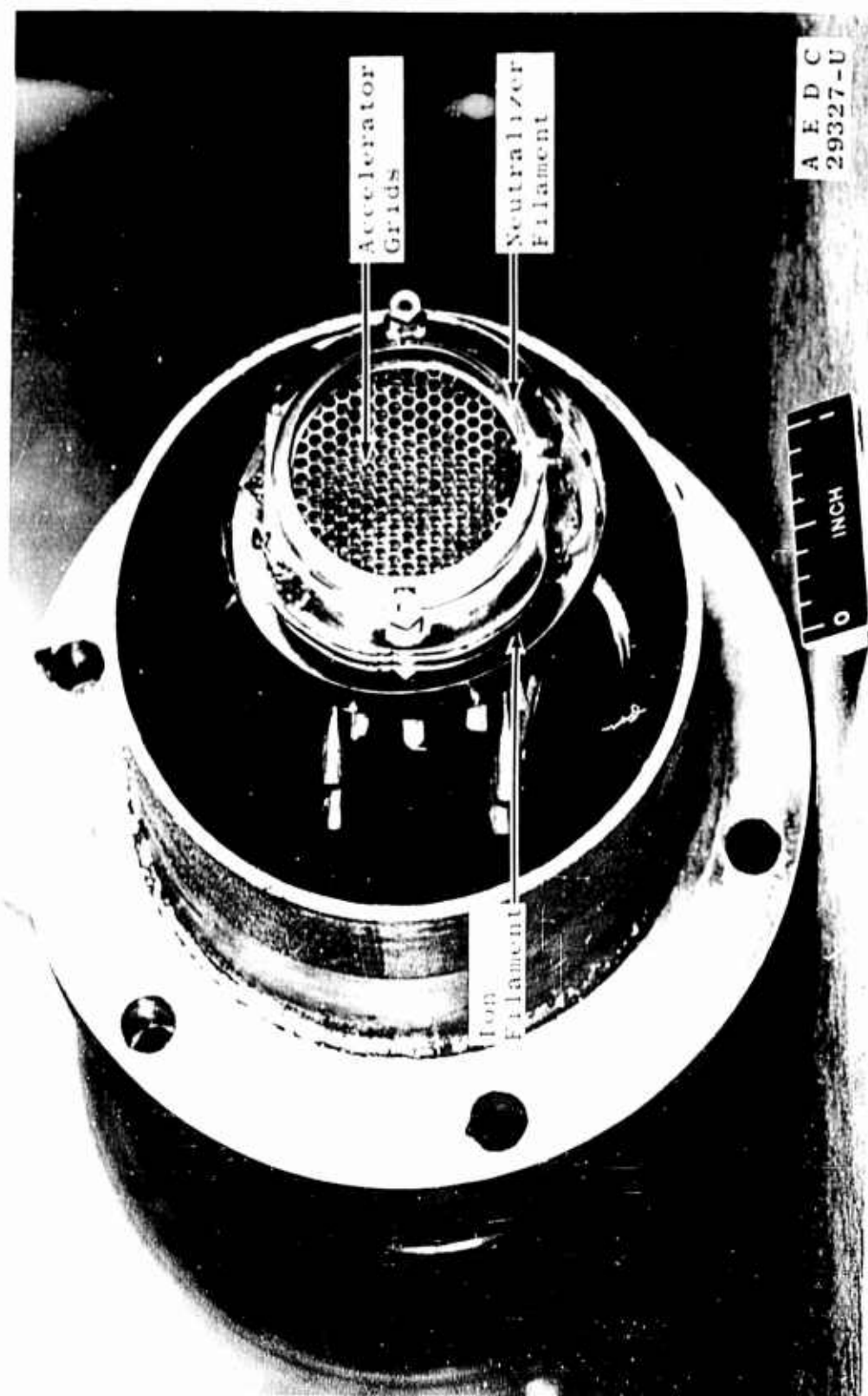


Fig. 1 Argon Discharge System Apparatus



a. End View
Fig. 2 Lithium Ion Gun



b. Three-quarter View
Fig. 2 Concluded

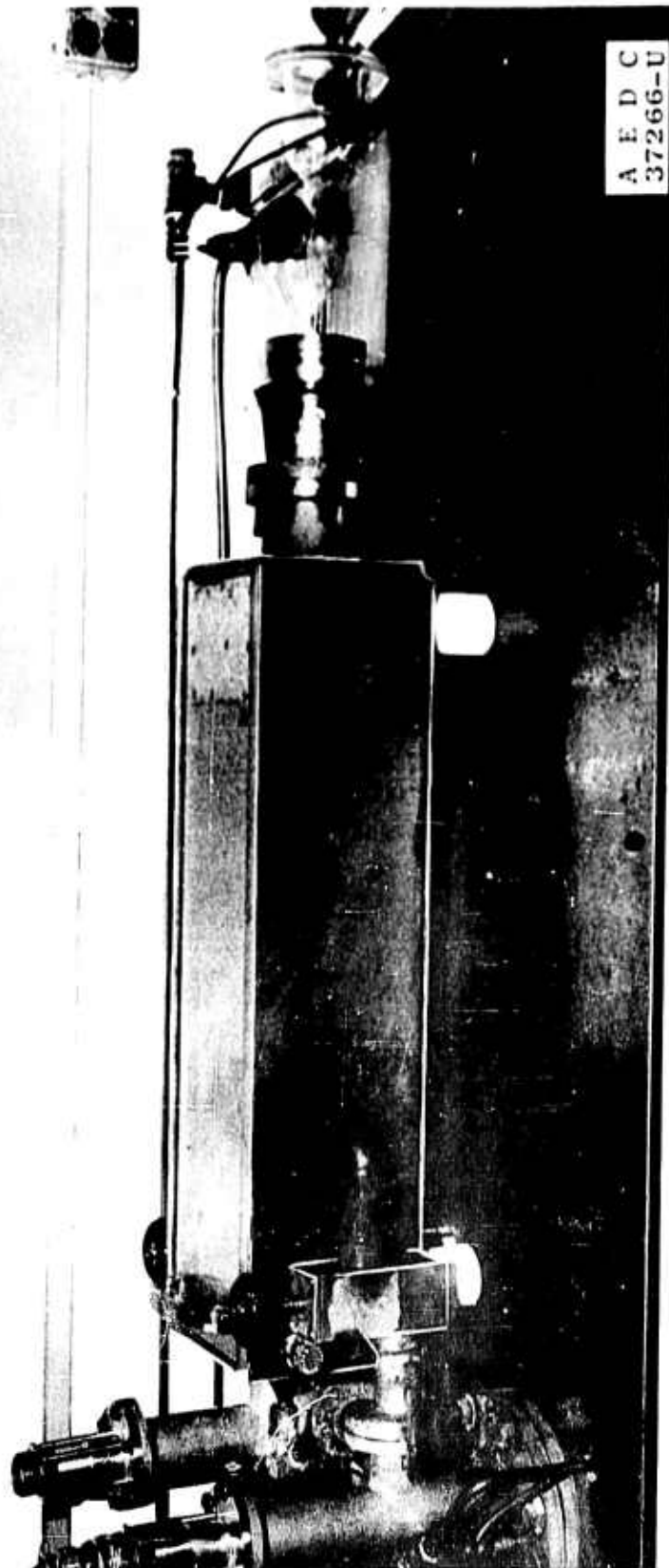


Fig. 3 Lithium Discharge System

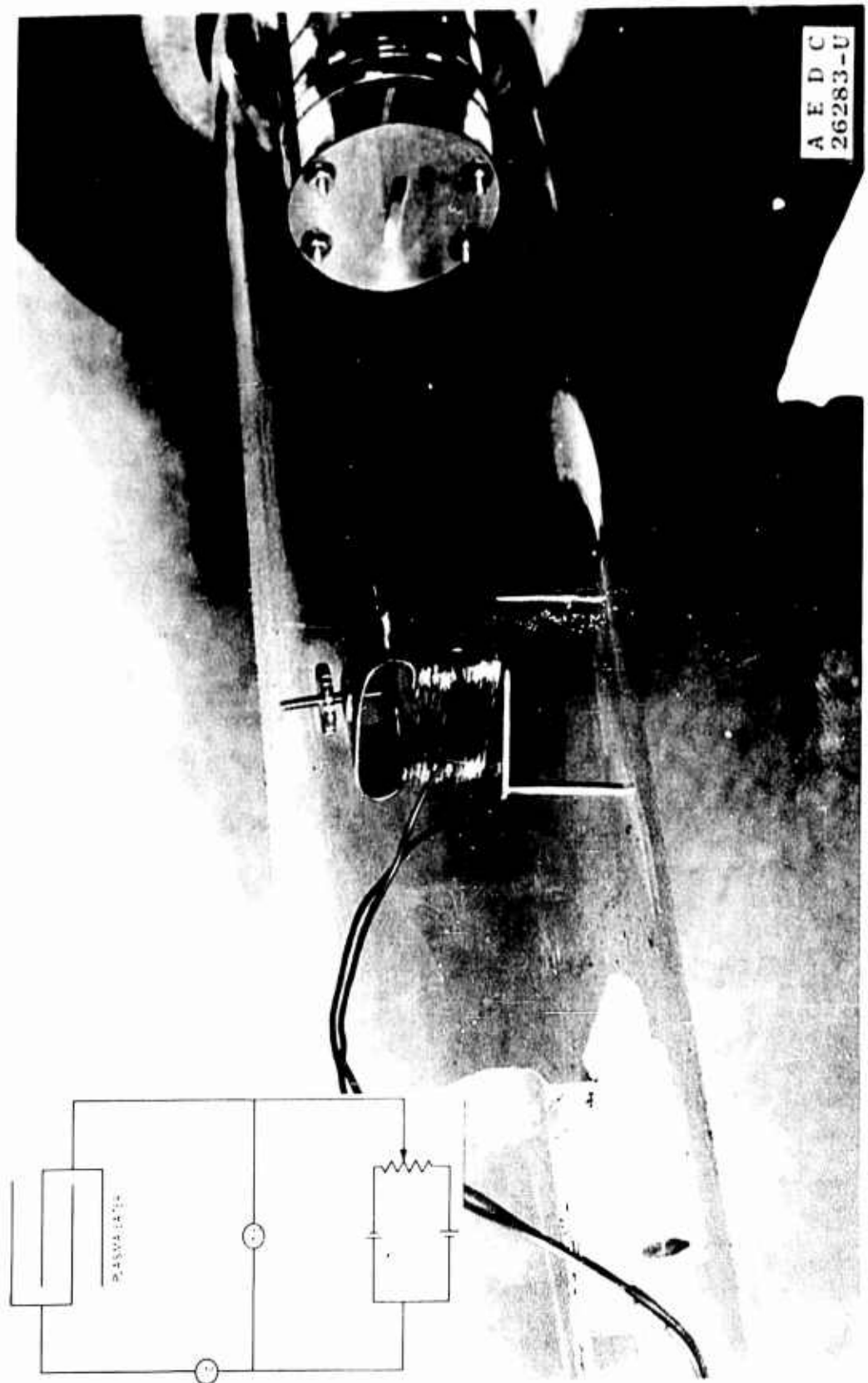


Fig. 4 Plasma Eater

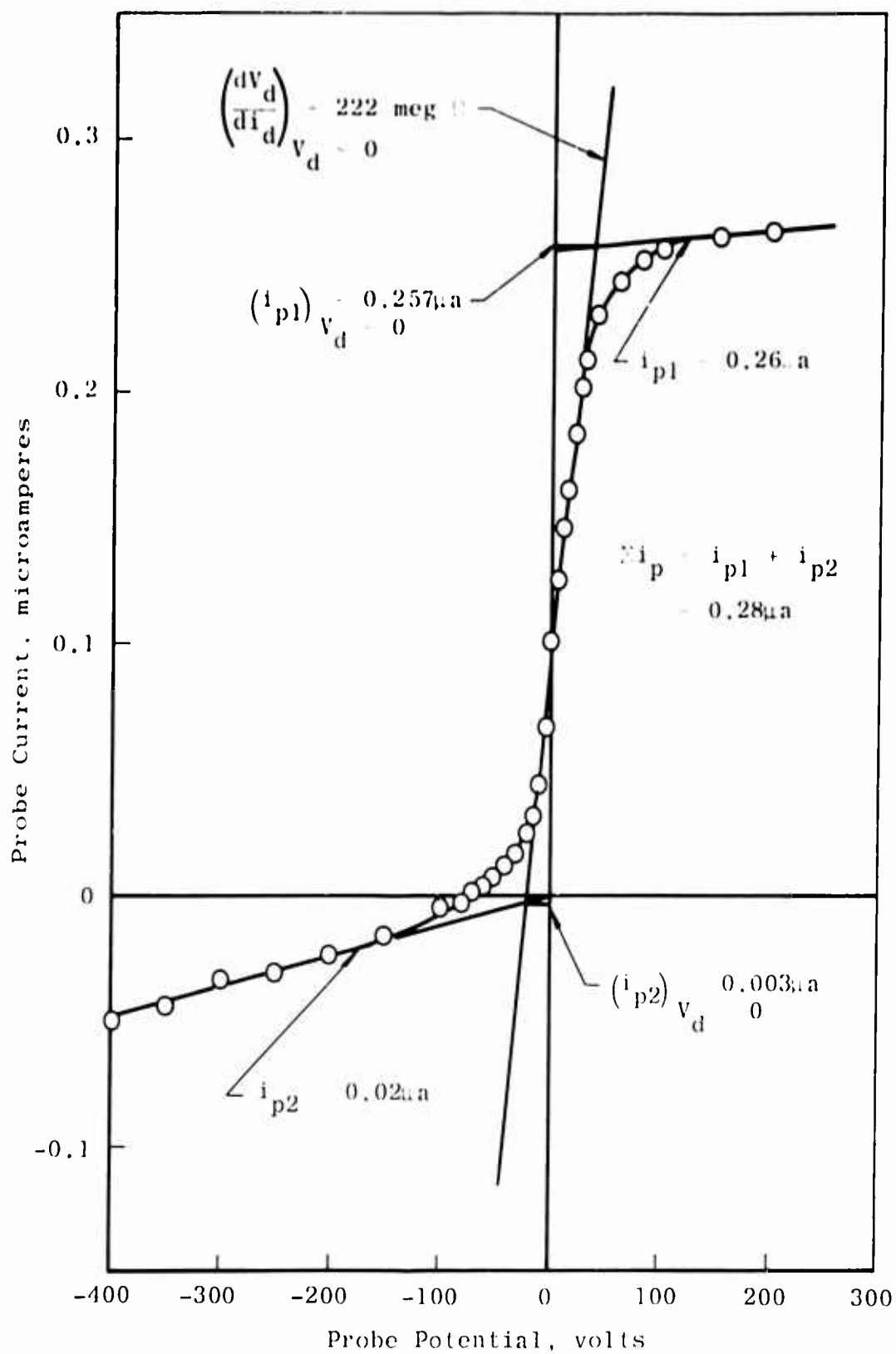


Fig. 5 Plasma Eater Characteristics

- J_{o1} - Electron space current in the plasma adjacent to plate No. 1
- J_{o2} - Electron space current in the plasma adjacent to plate No. 2
- V_1 - Plate to plasma potential, plate No. 1
- V_2 - Plate to plasma potential, plate No. 2
- V_c - Contact potential of plasma
- V_d - Probe voltage

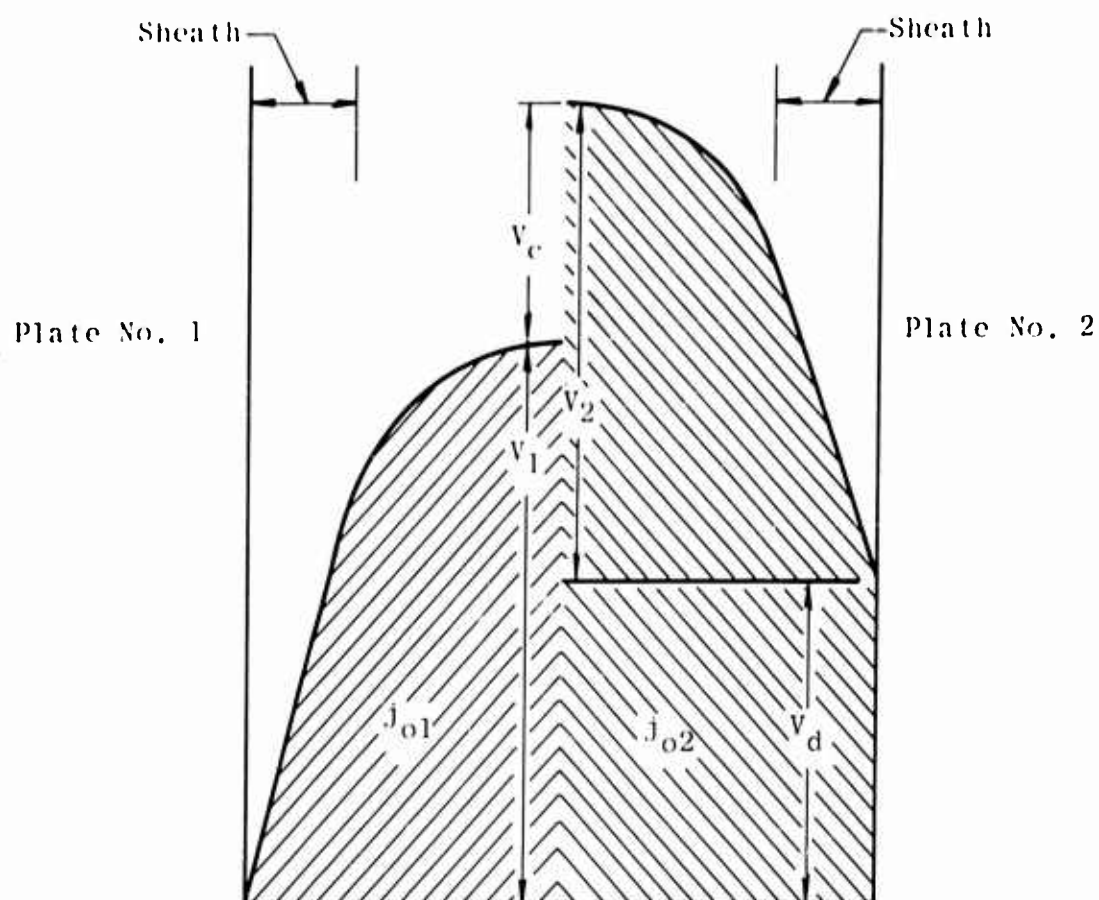


Fig. 6 General Potential Diagram between Plates

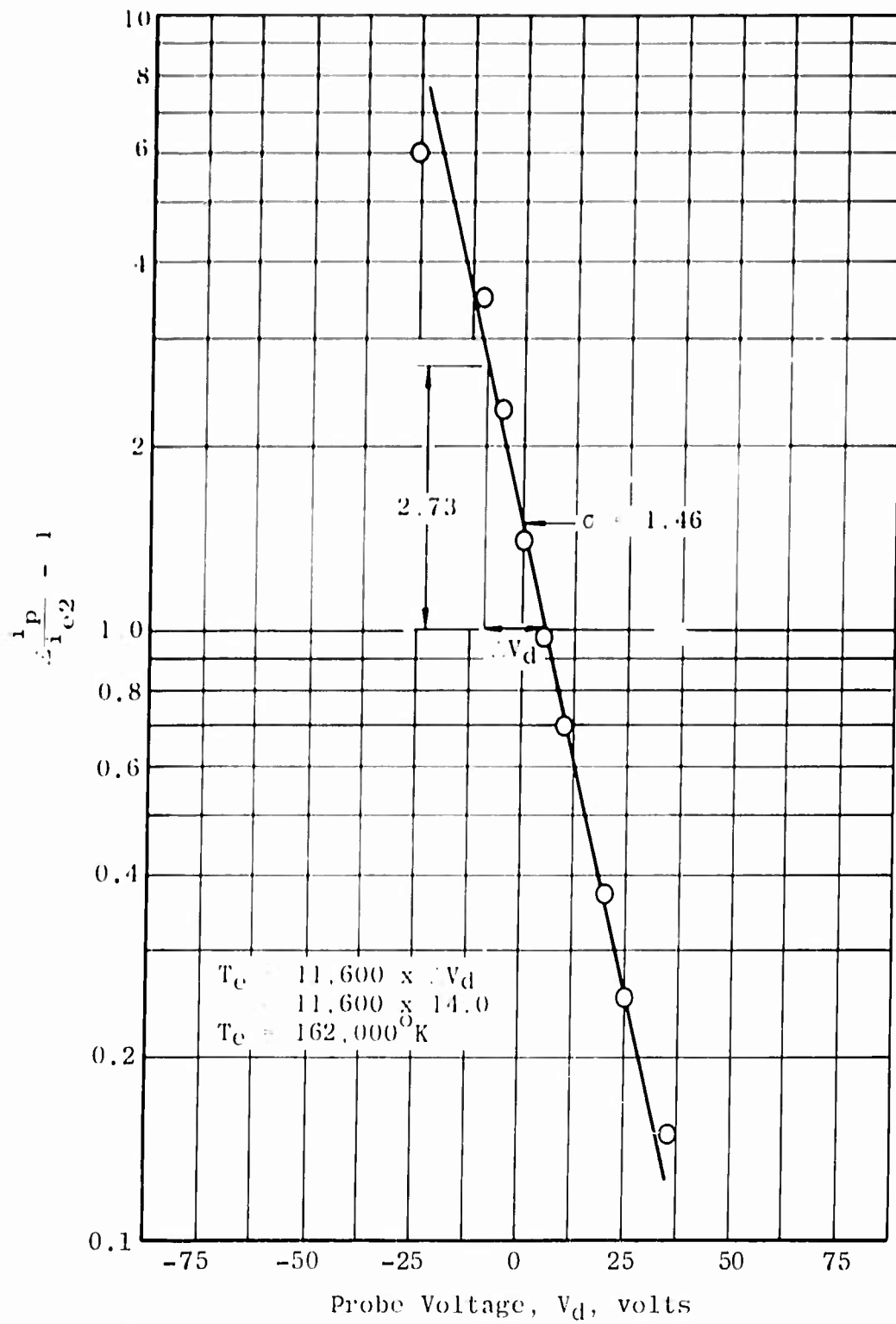


Fig. 7 $\frac{\sum i_p}{i_{e2}} - 1$ vs Probe Voltage

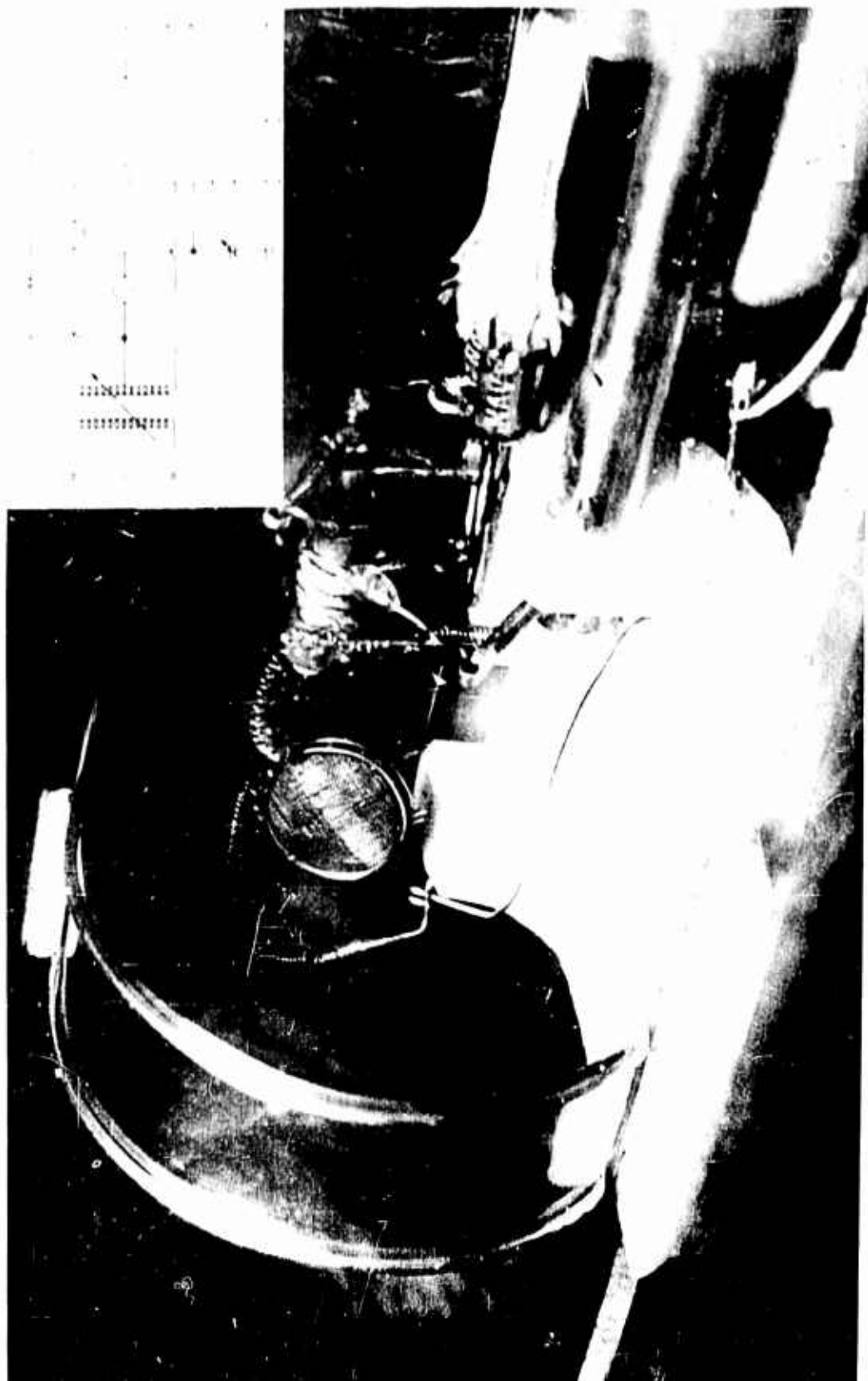


Fig. 8 Positive Ion Probe

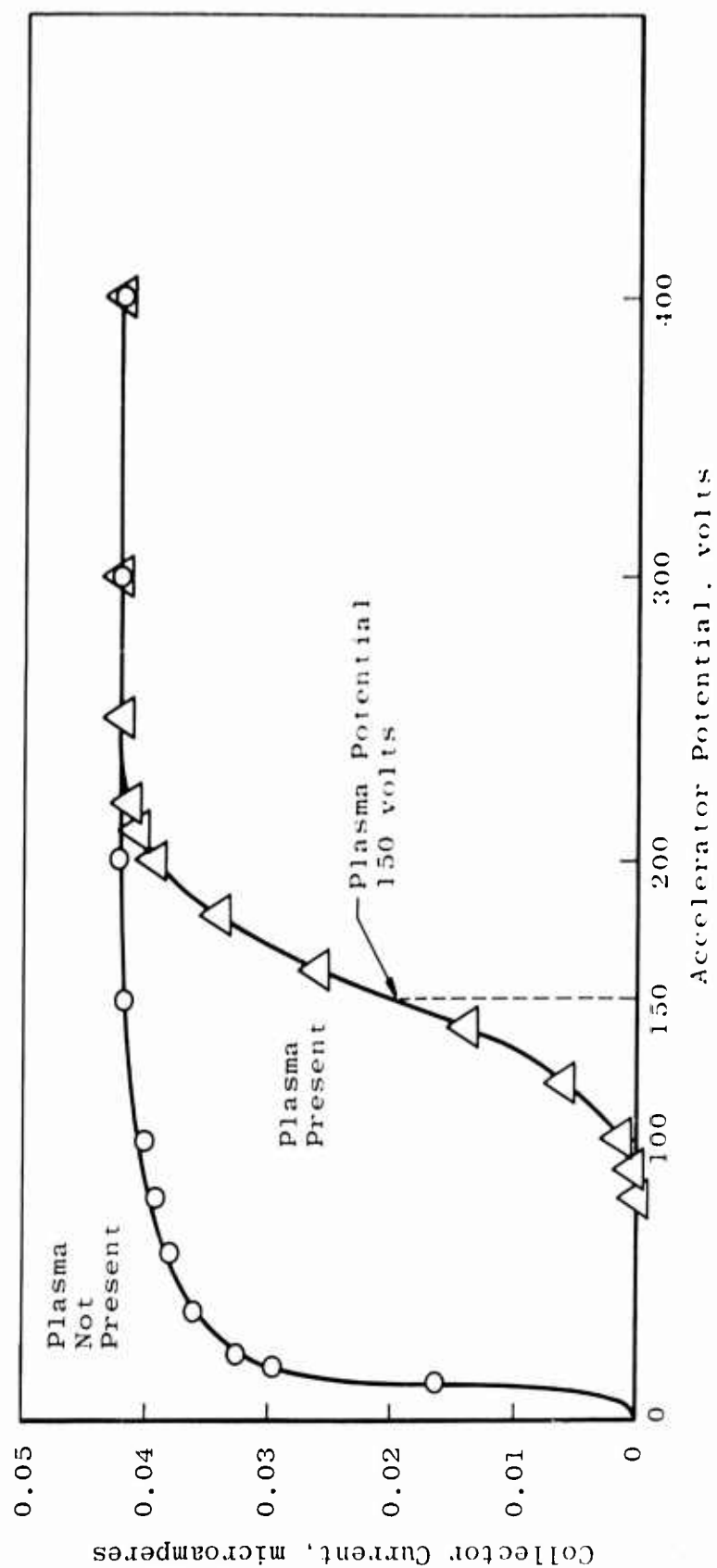


Fig. 9 Positive Ion Probe Characteristics

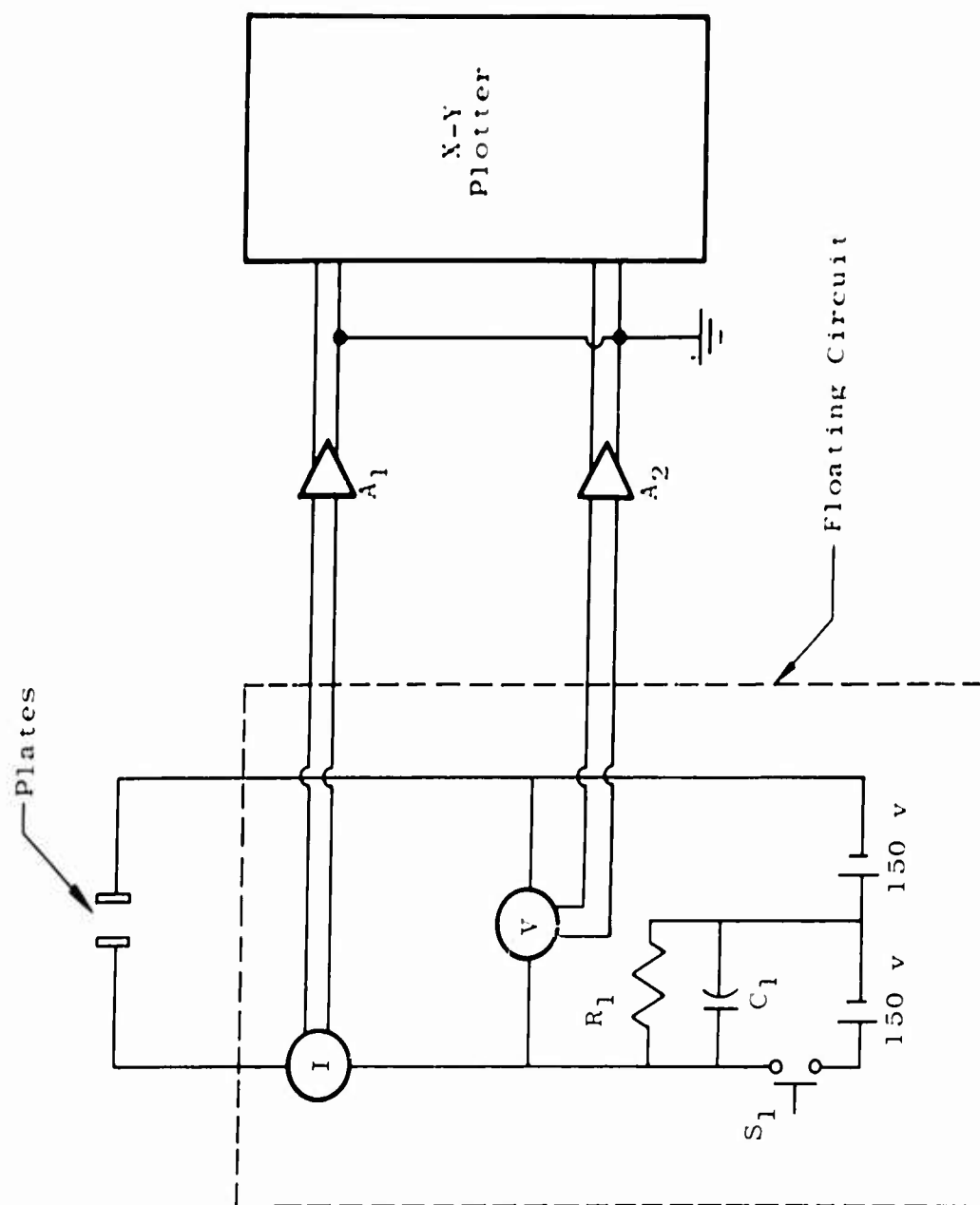


Fig. 10 Floating Double Probe Circuit

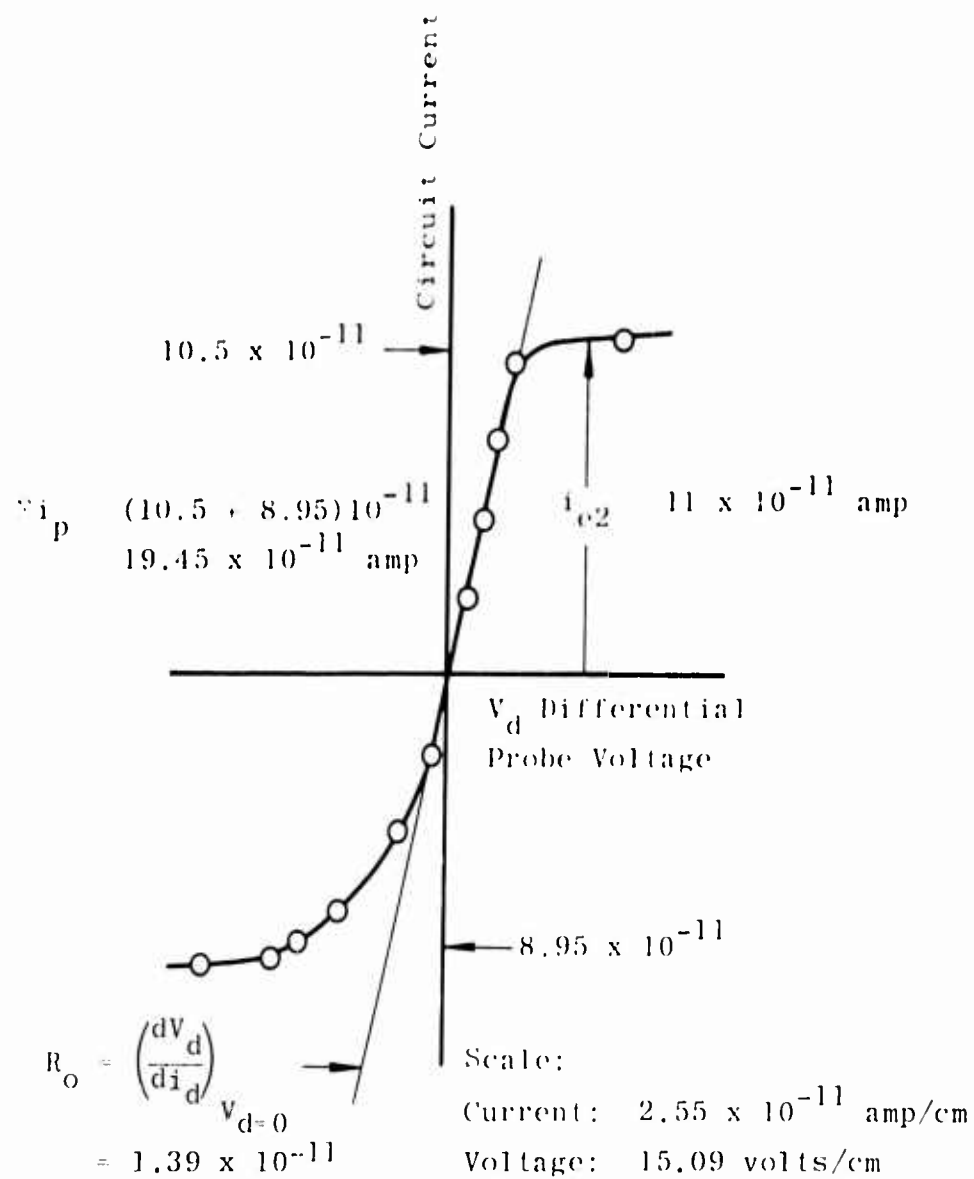


Fig. 11 Volt-Ampere Characteristic; Double Probe

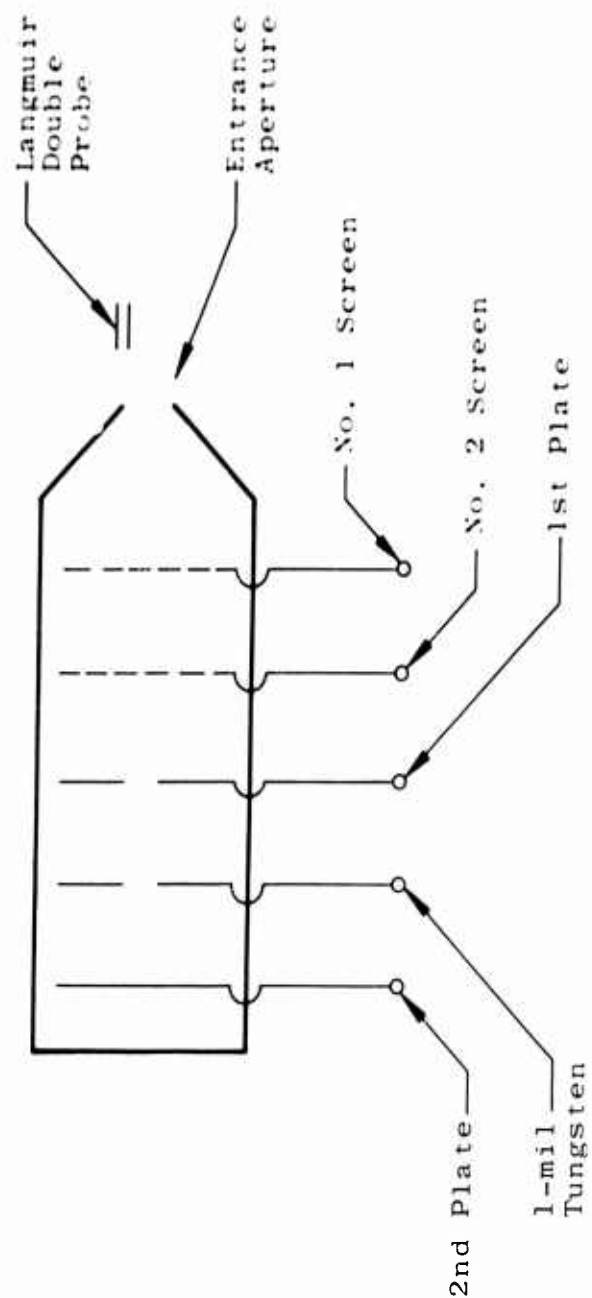


Fig. 12 Faraday Cup

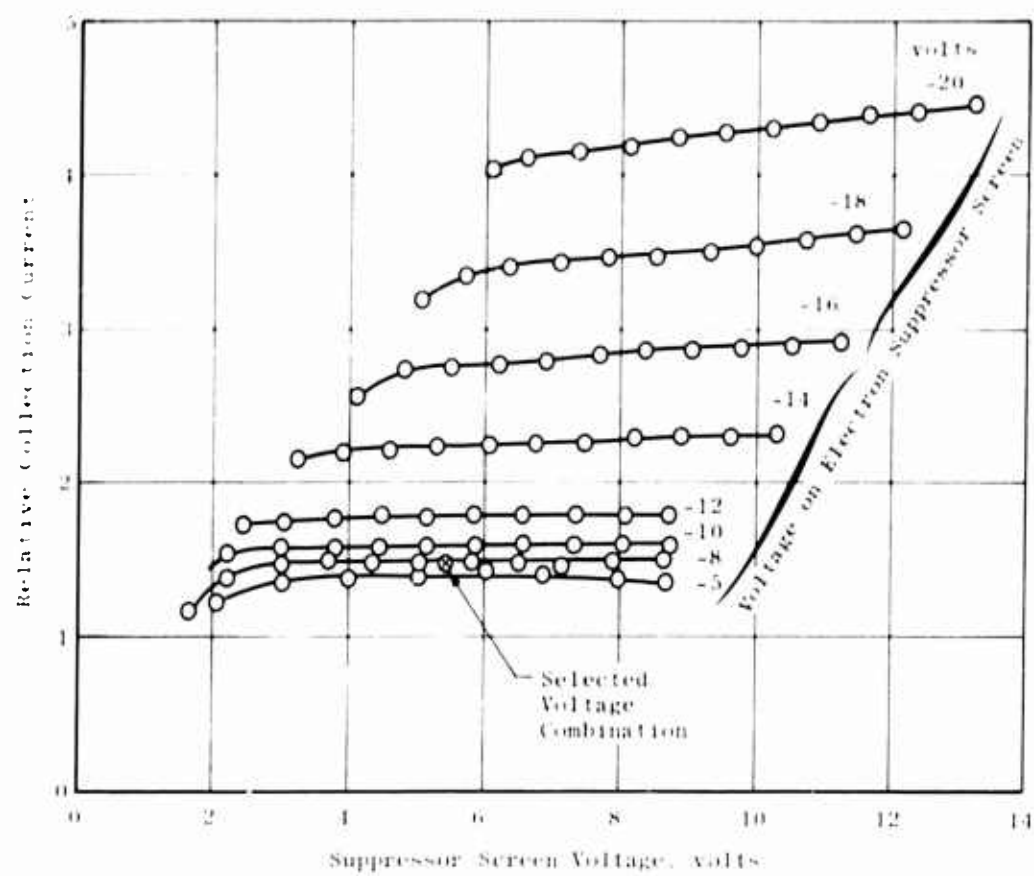
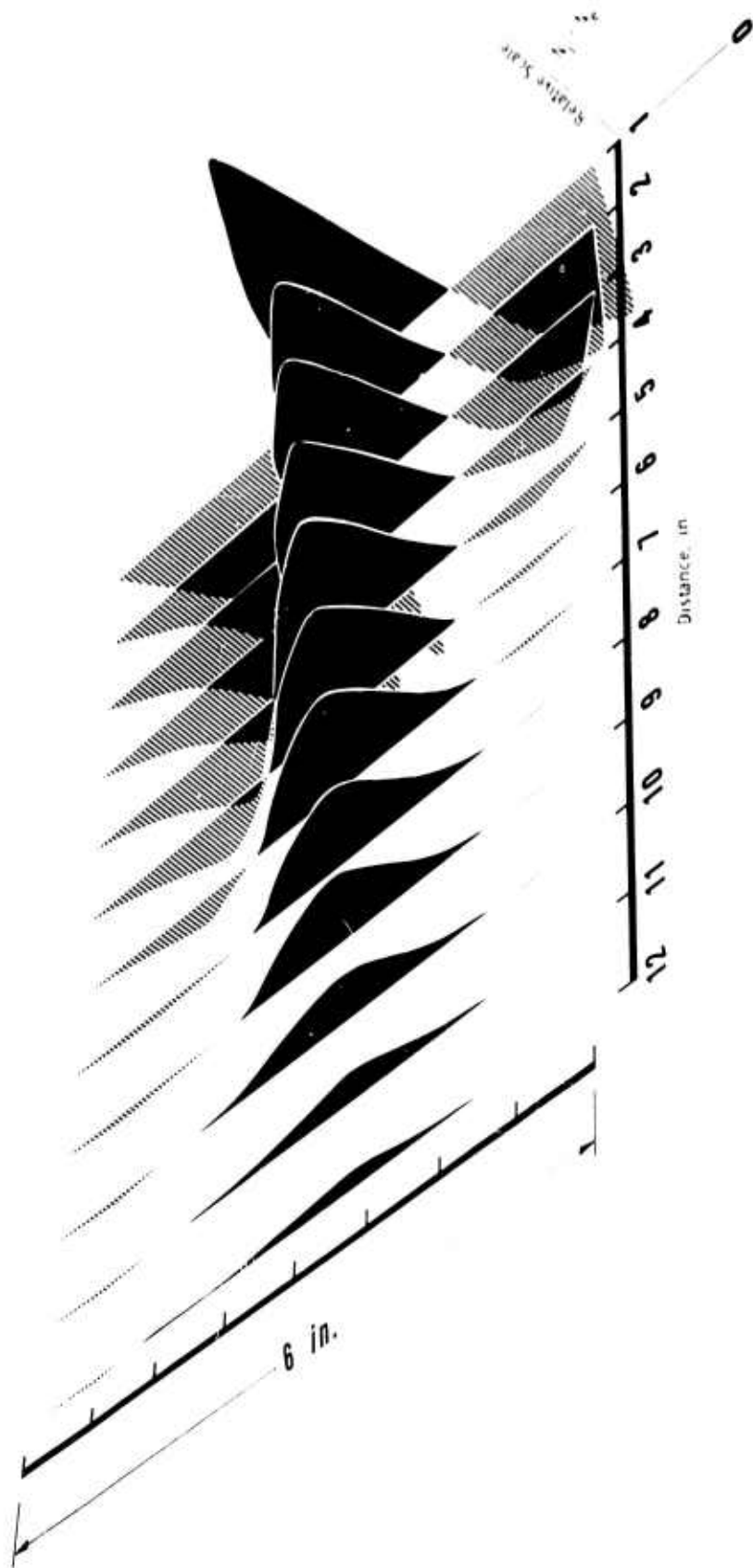
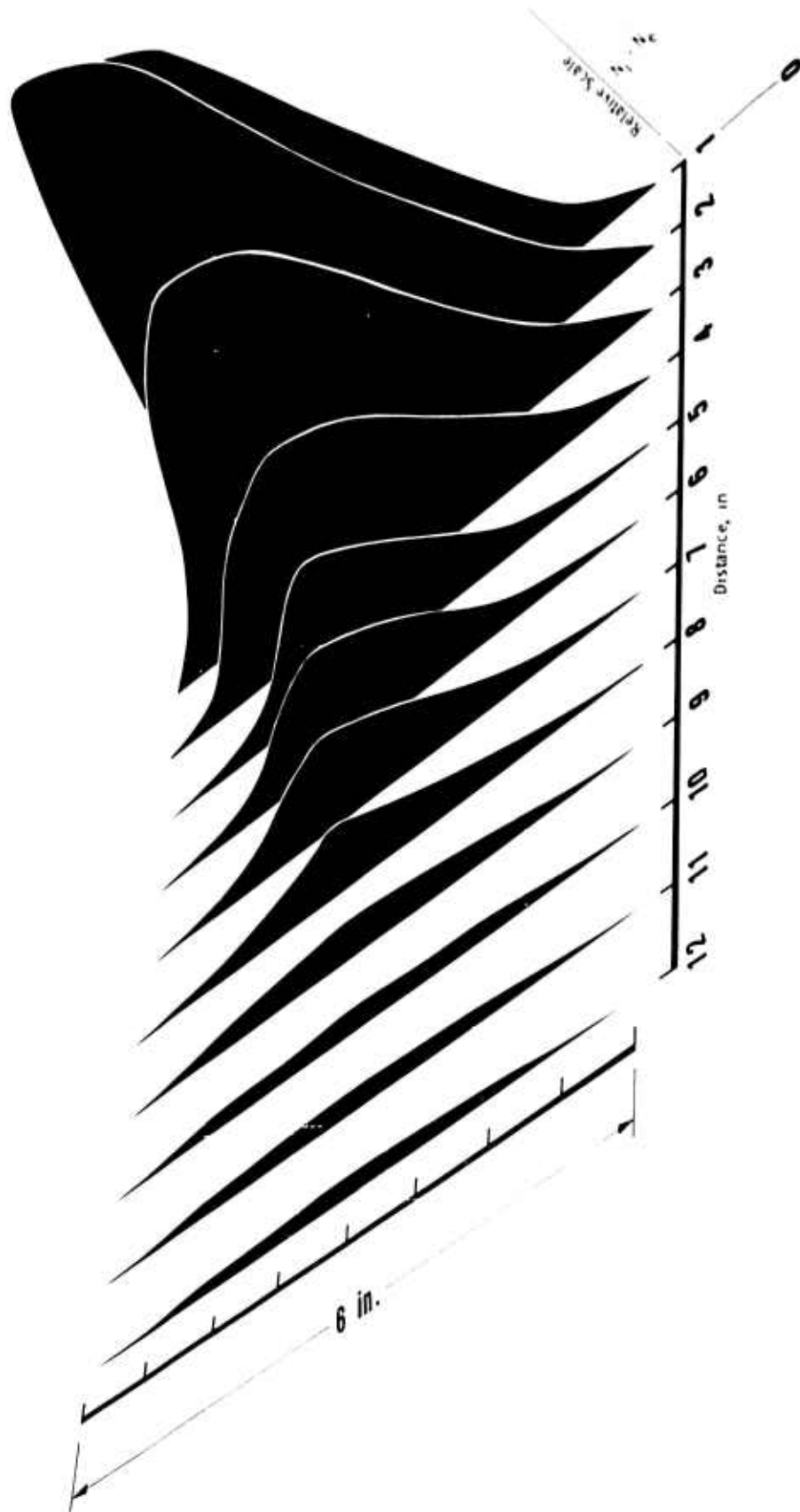


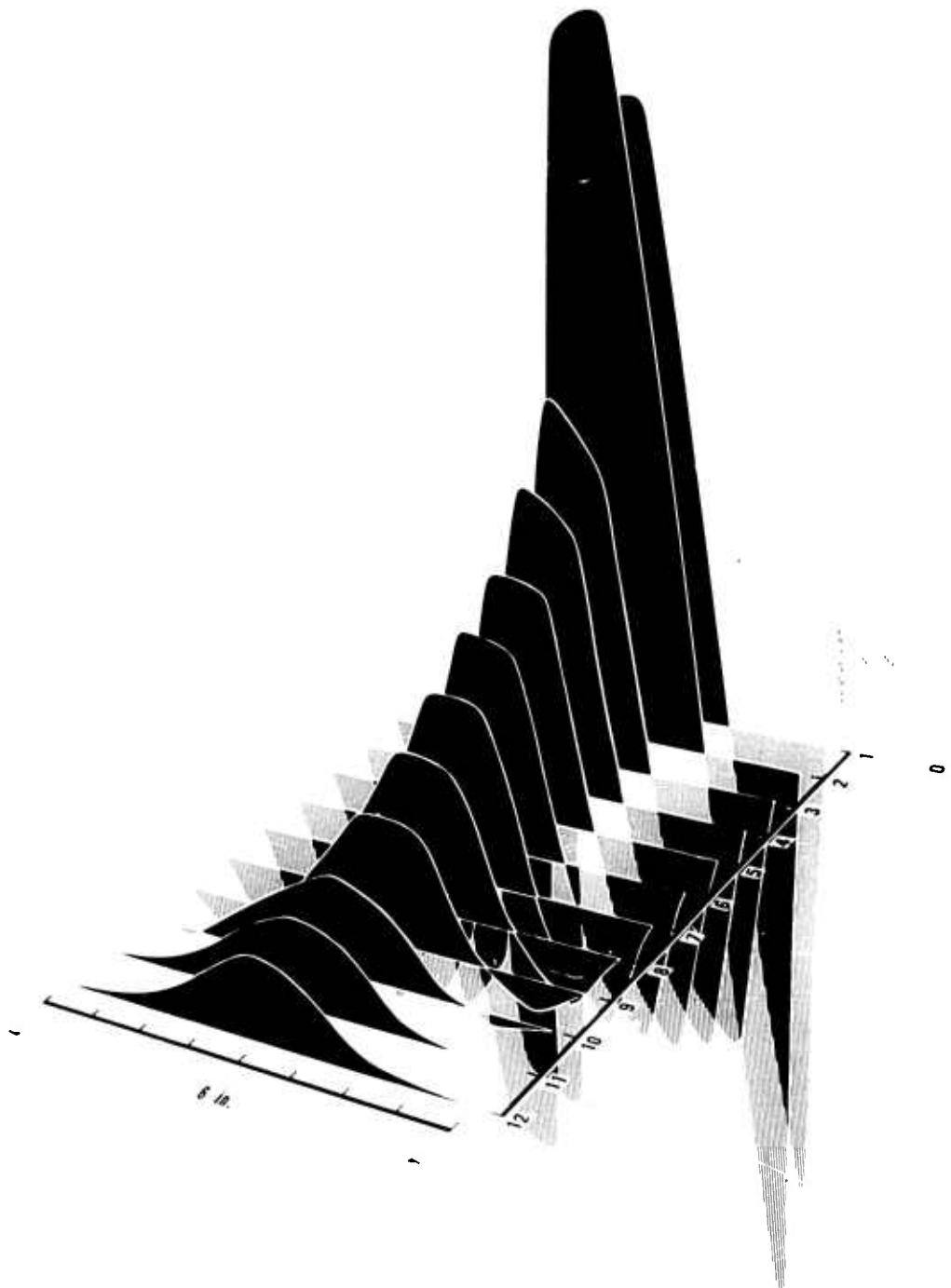
Fig. 13 Faraday Cup Biasing



a. Neutralizer On
Fig. 14 Chamber Grounded

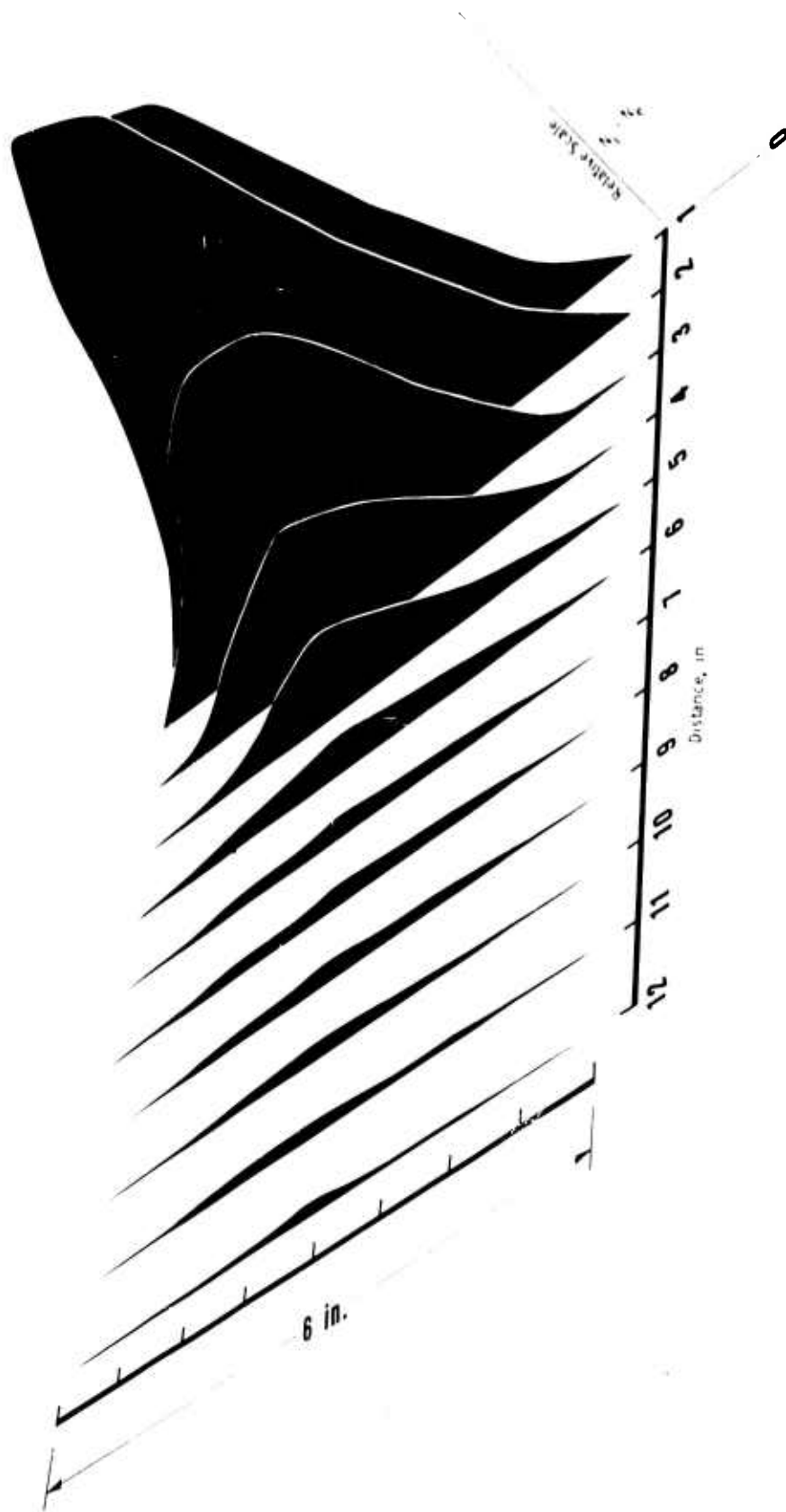


b. Neutralizer Off
Fig. 14 Concluded



a. Neutralizer On

Fig. 15 Chamber Floating



b. Neutralizer Off
Fig. 15 Concluded

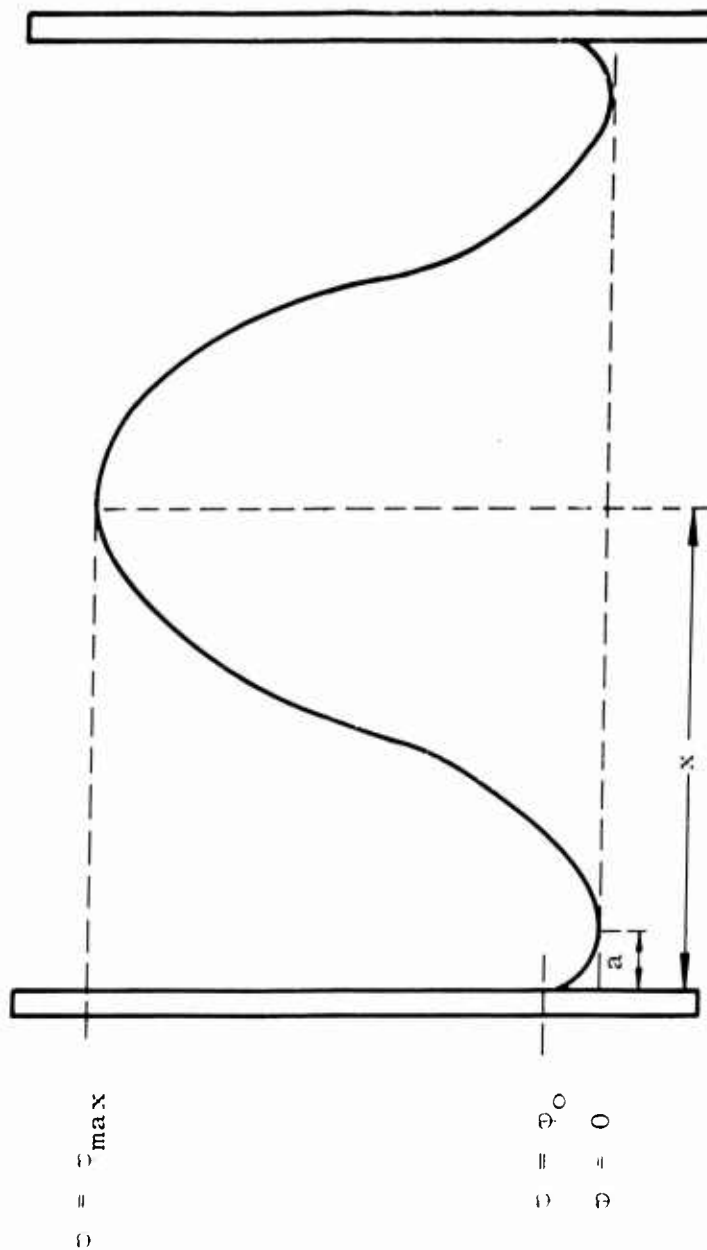


Fig. 16 Sample Potential Distribution

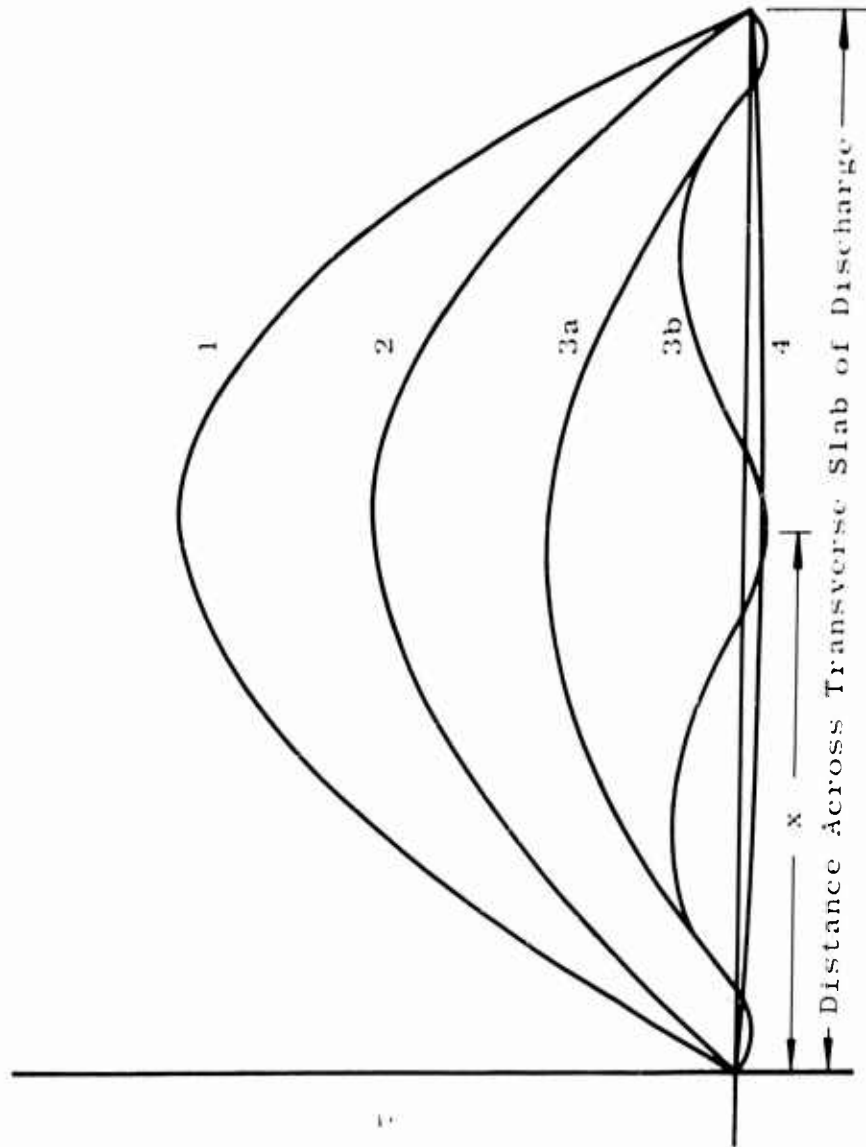


Fig. 17 Possible Potential Solutions, Eqs. (18) and (19)

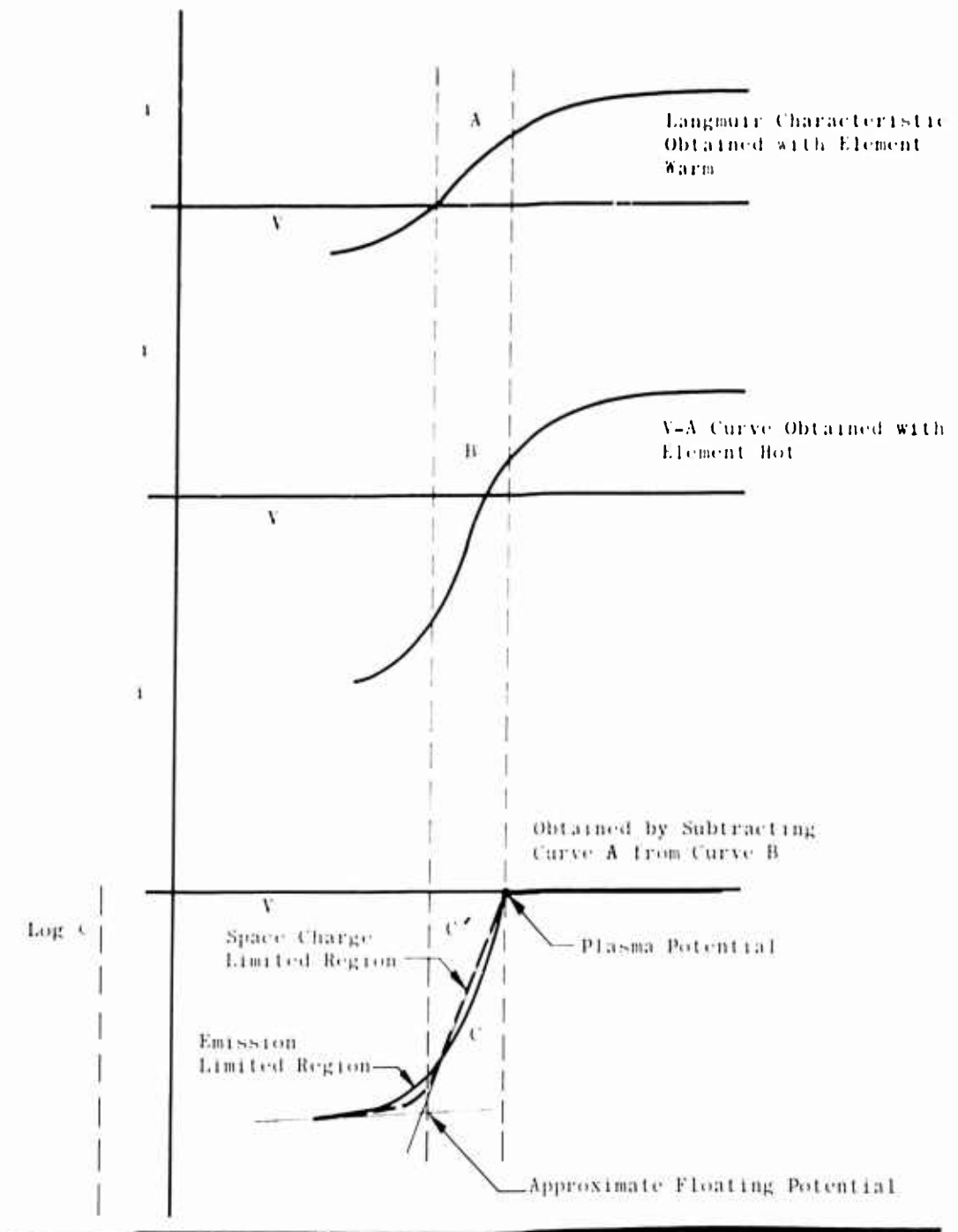


Fig. 18 Graphical Solution of Emissive Probe Data